Proceedings of the 17th World Congress
The International Federation of Automatic Control
Seoul, Korea, July 6-11, 2008

State and Ore Hardness Estimation in Semiautogenous Grinding ⋆

Alejandro Cuevas * **Aldo Cipriano** *

* *Department of Electrical Engineering,*
Pontificia Universidad Católica de Chile, Santiago, Chile
(e-mail: agcuevas@ing.puc.cl, aciprian@ing.puc.cl)

Abstract: Semiautogenous milling is difficult to control both because of its non-linear behavior and the effects of overloading due to increases in the ore charge or variations in ore characteristics. Advanced control strategies and operational change detection methods are thus in need of strengthening using techniques such as state estimation. Non-linear state estimation is a complex task for which various solutions have been proposed, such as the extended Kalman filter, the particle filter and the moving horizon estimator. In this study we present firstly a quantitative comparison of these solutions using a dynamic model validated with mill data. The results indicate that in addition to its lower computational requirements, the extended Kalman filter delivers the best performance in robustness and estimation error. Next, we propose a method for estimation of changes in the hardness of the ore feed that we test by simulation. Finally, we show that this method also works with real data.

Keywords: Semiautogenous grinding; State estimation; Extended Kalman filter; Particle filter; Moving horizon estimation; Genetic algorithms.

1. INTRODUCTION

Semiautogenous milling, one of the most widely used methods of ore concentration, involves the feeding of large rock particles and water into a grinding mill containing steel balls that rotates at approximately 75% of its critical speed. The slurry and ball charge adheres to the walls of the mill before cascading off at a given angle, causing impact and fragmenting the ore. This process exhibits significant non-linearities and can be adversely affected by mill overload, whether caused by an excess of ore or variations in its hardness or granulometry. In response, various advanced control algorithms have been developed to achieve a more robust operation of the process in the face of such variations or changes in the ore feed (Sbarbaro et al., 2005).

Advanced control and operational change detection systems generally employ process models. The most developed versions use relatively simple structures whose parameters are identified on the basis of input-output data. Others attempt to model the phenomenology of the process, but these are more complex designs based on fracture kinetics whose parameters include grinding and discharge rates (Austin, 1997). Although such models can reproduce the interactions between the variables more accurately, they require a non-linear state estimator for use in control or fault detection and diagnosis. Various solution alternatives are available for state estimation in non-linear systems, and their suitability must be evaluated case by case. In (Herbst et al., 1980), for example, a derivation of the Kalman filter known as the extended Kalman filter (EKF) is utilized in ball mill applications. More recent proposals include the use of particle filters (Arulampalam et al., 2002) and moving horizon estimation (Rao et al., 2003) for general application.

In this work we compare the three above-mentioned estimation methods using a dynamic semiautogenous grinding model developed in (Amestica et al., 1996) and (Gonzalez et al., 2006). The model was validated with operating data from a pilot plant. Our first objective is to compare state estimators on the grinding plant model. Our second objective is to identify hardness variations in the ore feed in real time. For these purposes we assume the presence of sensors that measure power consumption and total charge weight, from which we can deduce the discharge flow of water and ore. Input measurements are total ore feed flow, feed water flow and the ore's granulometric distribution.

2. DYNAMIC MODEL

The basic elements of a semiautogenous (SAG) mill are a grinding chamber, a discharge module and slurry transport, as depicted by the block diagram in figure 1. The ore feed is represented by vector f, whose components express the ore flow by size. F_a indicates the feed water flow.

The grinding chamber is a rotating cylinder where the actual grinding takes place both through collisions between the ore particles and the impact of the steel balls. Block C in figure 1 is a classifier consisting of a grate and a pulp lifter that distributes the slurry into flows either for immediate discharge or recirculation to the chamber and further grinding. The dynamic model of the mill we will employ here is the one given in (Amestica et al., 1996). It consists of the following variables and parameters:

⋆ This work was supported by Fondecyt Project No. 1050684 and the Pontificia Universidad Católica de Chile

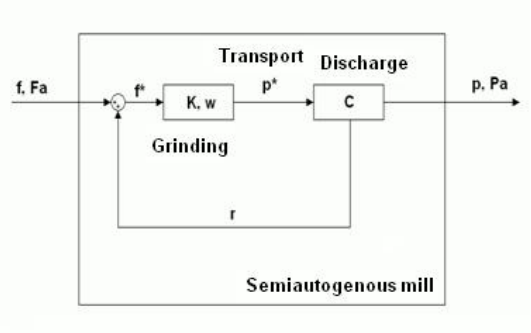

Fig. 1. Block diagram of SAG system.

- Variables

f_i,F_a:	Ore feed flow by size class, feed water flow.
F_M:	Total mass flow.
w_i,W_A:	Ore mass by size interval, water mass.
W_M:	Total ore mass inside mill chamber.
p_i,P_A:	Discharge mass flow by size class, water flow.
P_M:	Total ore mass flow.
f_i^*:	Ore mass flow by size class entering mill chamber.
p_i^*:	Discharge mass flow by size class exiting mill chamber.
r_i:	Ore mass flow by size class for internal recirculation.
J:	Load fraction of mill chamber.
M_p:	Mill power consumption.

- Parameters

K:	Ore grinding rate by size class.
C:	Classification efficiency at discharge grate.
P^*:	Internal mass flow.
γ_A:	Water discharge rate.

All flows are measured in T/h and masses in T . Mill power is measured in kW .

The equations defining the model are categorized into grinding (1), transport (2) and classification equations (3):

$$\frac{dW_{i+1}}{dt} = K_i w_{i+1} \tag{1}$$

$$p_i^* = \frac{P^*}{W_m} w_i \tag{2}$$

$$r_i = \frac{P^*}{W_m} C w_i \; ; \; p_i = \frac{P^*}{W_m}(I_n - C) w_i \tag{3}$$

Parameters γ_A and P^* vary with time and are obtained from measurements while matrices K and C are derived from a probability distribution of the reduction and classification phenomena (Austin, 1997). Parameters γ_A and P^* satisfy the following relationships:

$$\gamma_A = r + \frac{s}{W_m^4} \; ; \; P^* = q\sqrt{W_m} \tag{4}$$

where r, s and q are calibration parameters.

The dynamic model synthesizing mill operation takes into account the steel balls that increase the effectiveness of the grinding process. In simplified models, the grinding phenomena that reduce particle size can be represented by a single parameter known as the effective ore grinding rate K. If we denote the ore mass greater than size d_i in the chamber as W_{i+1}, and if K_i is the effective grinding rate for ore of size d_i, we have the grinding relationship given by (1).

Power consumption and load fraction variables are closely related. For the mill we are modeling, load fraction (from 0 to 1) has been found experimentally to satisfy the following relationship:

$$J = aW_m + b \tag{5}$$

where W_m is derived from the density and porosity of the ore. The additive constant W_b represents the volume of the steel balls.

As for power consumption, it is given by the mill parameters and the total mass inside the chamber:

$$M_p = (mJ + c)\,(W - m + W_A + W_b) \tag{6}$$

Coefficients a, b, m and c are also calibration parameters. All parameters values are displayed in Table 1.

Table 1: Calibration parameters of models.

a	b	m	c	r	s	q	W_b T
0.407	0.0723	-24.3	18.6	16.86	0.102	29	0.52

The equations given above are combined in the state equations as:

$$\frac{dw_i}{dt} = -\frac{1}{W_m}\left[P^*\,(I_n - C') + M_p R^{-1} K^e R\right] w_i + f_i \tag{7}$$

$$\frac{dW_A}{dt} = -\gamma_A W_A + F_A \tag{8}$$

where i is the ore size class index, C' is defined to include the recirculation flow and K^e is the specified grinding rate related to power consumption M_p. R is a ones and zeros matrix wich relates w_i with W_i. The outputs defined in the model can be measured or inferred from operation data and are given by:

$$\begin{aligned} p_i &= \frac{P^*}{W_m}\,(I_n - C)\,w_i \\ P_M &= \sum_{i=1}^{n} \frac{P^*}{W_m}\,(I_n - C)\,w_i \\ P_A &= \gamma_A W_A \end{aligned} \tag{9}$$

This base model incorporates $n = 26$ size classes and was calibrated with data obtained from a pilot plant run by Codelco (Amestica et al., 1996).

3. SIMULATION

The simulation was carried out in Simulink. Since the model is continuous, it was discretized using $\Delta t = 10\ s$ as a step in its integration, with (7),(8) as the state functions and (9) as the output function in their discretized forms. The initial operating conditions were 8.4 T/h for total ore feed flow (4.2 T/h hard and 4.2 T/h soft ore) and 1.2 T/h water feed flow.

Figure 2 shows the trend over time of hold-up mass and mill power consumption over a period of 5 h. Total feed flow was increased by 25% at $t = 2\ h$, the ore fines proportion was varied from 80% to 95% at $t = 3\ h$, and finally, soft ore was varied from 60% to 20% at $t = 4\ h$. Note that an increase in total feed flow leads to a rise in total hold-up mass and therefore also in power consumption. If the total charge exceeds a certain threshold, the mill

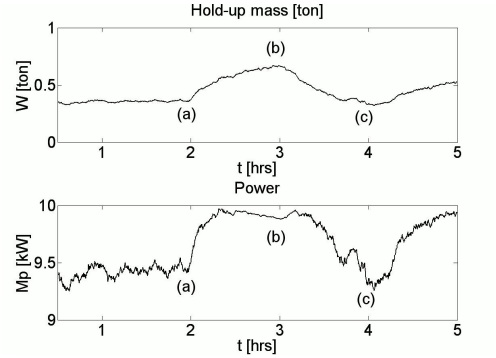

Fig. 2. Variation over time of hold-up mass and power due to changes in tonnage (a), granulometry (b) and hardness (c) of mill feed.

chamber becomes overloaded and breakage declines due to the excess ore, thus lowering the mill's power draw. If, on the other hand, the proportion of fines increases, both the load and the draw diminish due to the greater ease of ore evacuation. Finally, a lower soft ore proportion implies less breakage and therefore lower ore evacuation, thus increasing both load and power draw. For these reasons, a linear filter could not show satisfactory results as non linear estimations shown in the next section.

4. STATE ESTIMATION

We now turn to the quantitative comparisons of the three state estimation solutions, they being the extended Kalman filter (Welch and Bishop, 2004), the particle filter (Arulampalam et al., 2002) and the moving horizon estimator (Rao et al., 2003).

For the extended Kalman filter (EKF), we used matrices Q and R , both dimension 5×5, which are equal to the identity matrix multiplied by a scalar for all states, which represents typical sensor noise or process noise. In the case of the particle filter (PF) we utilized $N_p = 20$, because better results didnt appear with larger number of particles. Finally, for the moving horizon estimator (MHE) a horizon of 5 and a time estimation step $\Delta t = 50$ were employed. Genetic algorithms were applied to solve the optimization problem, with 10 generations of 30 individuals initially distributed uniformly. The results of the search were then used as the starting solution in a classic optimization algorithm. A simplified version of the model was employed using the same structure but only five states: coarse-hard w_1, coarse-soft w_2, fine-hard w_3, fine-soft w_4, and water W_A.

$$\begin{aligned}
\frac{dw_1}{dt} &= -\frac{G_1 M_p}{W_m} w_1 + (1-\alpha)(1-\beta) F_m + \delta w_1 \\
\frac{dw_2}{dt} &= -\frac{G_2 M_p}{W_m} w_2 + \alpha (1-\beta) F_m + \delta w_2 \\
\frac{dw_3}{dt} &= -P_{m1} + \frac{G_1 M_p}{W_m} w_1 + (1-\alpha)\beta F_m + \delta w_3 \quad (10) \\
\frac{dw_4}{dt} &= -P_{m2} + \frac{G_2 M_p}{W_m} w_2 + \alpha\beta F_m + \delta w_4 \\
\frac{dW_A}{dt} &= -\gamma_A W_A + F_A + \delta W_A
\end{aligned}$$

Where δw_1, δw_2, δw_3, δw_4, δW_A are process noises of their respective state variables. G_1 is hard ore's hardness and G_2 is soft ore's hardness. Values of $G_1 = 0.1\ T/kJ$ and $G_2 = 0.2\ T/kJ$ are used, which represent averages for K matrix values for soft mineral and hard mineral, respectively.

Parameter β is defined as the ore fines mass flow proportion with respect to the total feed mass flow. Parameter α is defined as soft ore mass flow proportion with respect to the same total. Thus, $\alpha = 0$ indicates that the feed includes only hard ore, $\alpha = 1$ means it contains only soft ore and $\alpha = 0.5$ designates equal proportions of both. Therefore, α represents the overall hardness of the system in a single parameter.

The performance of the three estimators is summarized in Tables 2, 3 and 4 for the various operating scenarios. Root Mean Square Errors from the estimations are shown for the following ore variables: coarse $(w_1 + w_2)$, fine $(w_3 + w_4)$, hard $(w_1 + w_3)$, and soft $(w_2 + w_4)$. Table 2 gives the results for normal operating conditions, with total ore feed of 7 T/h, feed water flow of 1.2 T/h, fines proportion $\beta = 0.8$ and soft ore proportion $\alpha = 0.5$. In Table 3, we again have $\alpha = 0.5$, total ore feed of 7 T/h and feed water flow of 1.2 T/h, but $\beta = 0.9$. At $t = 2$ h total ore feed was increased 10%, and at $t = 4$ h, ore fines β were increased from 90% to 95% of feed flow. The operating conditions for Table 4 are normal with the exception that 10% more feed water flow was added at $t = 2$ h.

Table 2: RMSE in T for estimates under normal operating conditions.

	Coarse $w_1 + w_2$	Fine $w_3 + w_4$	Hard $w_1 + w_3$	Soft $w_2 + w_4$
EKF	0.0060	0.0081	0.0107	0.0028
PF	0.0082	0.0069	0.0072	0.0034
MHE	0.0162	0.0111	0.0370	0.0212

Table 3: RMSE in T for estimates with changes in tonnage and granulometry.

	Coarse $w_1 + w_2$	Fine $w_3 + w_4$	Hard $w_1 + w_3$	Soft $w_2 + w_4$
EKF	0.0053	0.0064	0.0162	0.0124
PF	0.0081	0.0069	0.0071	0.0032
MHE	0.0026	0.0131	0.0075	0.0094

Table 4: RMSE in T for estimates with changes in feed water flow.

	Coarse $w_1 + w_2$	Fine $w_3 + w_4$	Hard $w_1 + w_3$	Soft $w_2 + w_4$
EKF	0.0059	0.0082	0.0108	0.0028
PF	0.0114	0.0080	0.0108	0.0050
MHE	0.0159	0.0113	0.0367	0.0211

Figures 3, 4 and 5 graph the variation over time of the state and state estimates. The operation conditions are the same as in Table 3. The estimations are implemented using (10) as a simplified model of the 26 states model from which the measures are obtained. Initial estimations are 0.05 T for coarse, 0.15 T for fine, hard and soft, picked as a normal operation. The tests reveal that the estimators generally behave well in the face of various types of disturbances relative to normal operation, with EKF and PF giving similar results and MHE slightly worse. They do not seem to be strongly affected by operating changes, and thus

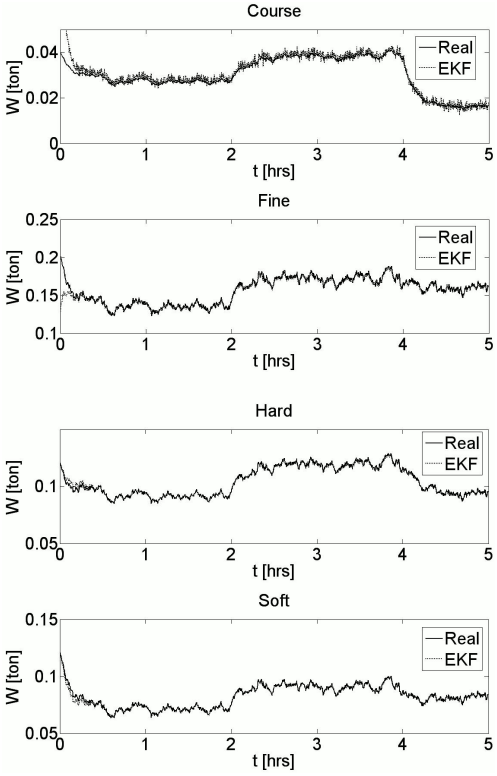

Fig. 3. State and state estimates with EKF.

would be attractive for use with processes such as the one studied here.

5. HARDNESS ESTIMATION

5.1 Joint state-parameter estimation

In our model (10) a change in ore hardness is represented by a single parameter α. The online estimation of the hardness of the ore in the system will therefore also require the estimation of the state.

The joint state-parameter estimation can be set out as follows: given known measurements (P_m, P_A, J and M_p), and inputs (F_M, F_A, β), estimate the unknown parameter α and the state given by w_1, w_2, w_3, w_4, W_A.

To solve this problem we resort to an EKF given that for joint estimation it exhibits not only the best performance, but also more robustness with respect to PF in distinct scenarios. The parameter α is added as a new state to (10), which models its variation over time:

$$\alpha_{k+1} = \alpha_k + \eta_k \tag{11}$$

where η_k is the noise term whose variance is σ_η . Appropriate tuning of the will yield good results for the estimates of α.

5.2 Results of the joint estimation

To evaluate the method just proposed we performed a joint state-parameter estimation in a simulation with the following characteristics: At $t = 2\ h$ the soft ore in the defined feed $[f_i, F_A]$ was varied from 20% to 40%, and at $t = 4\ h$ the fines in the total feed flow was increased from

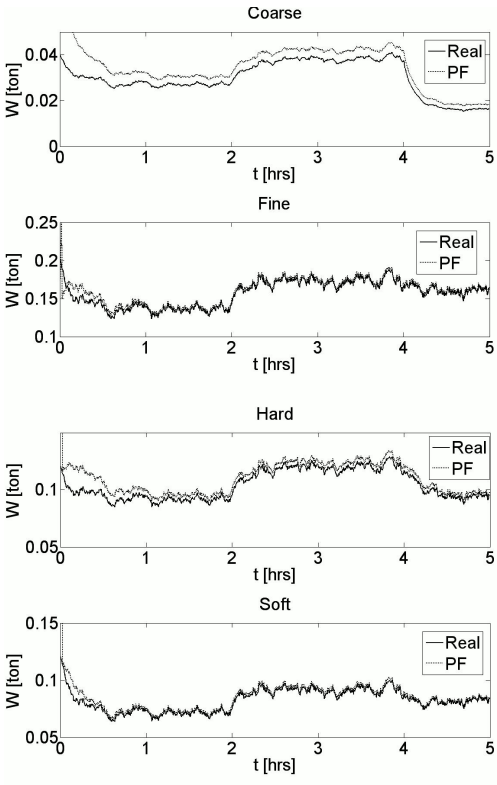

Fig. 4. State and state estimates with PF.

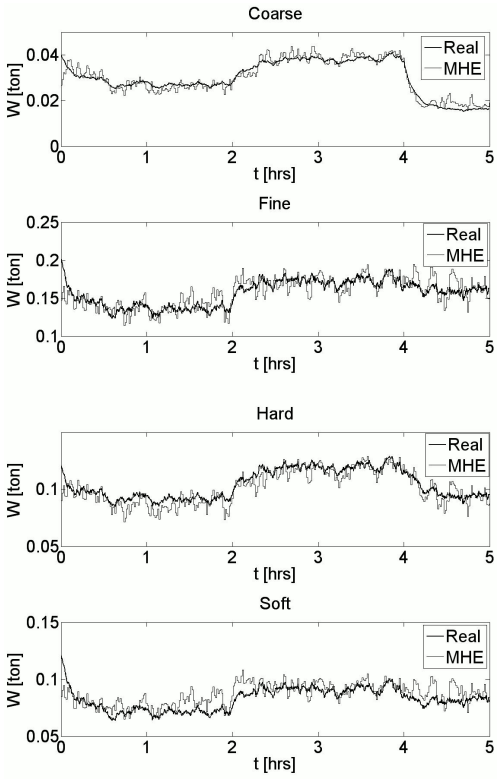

Fig. 5. State and state estimates with MHE.

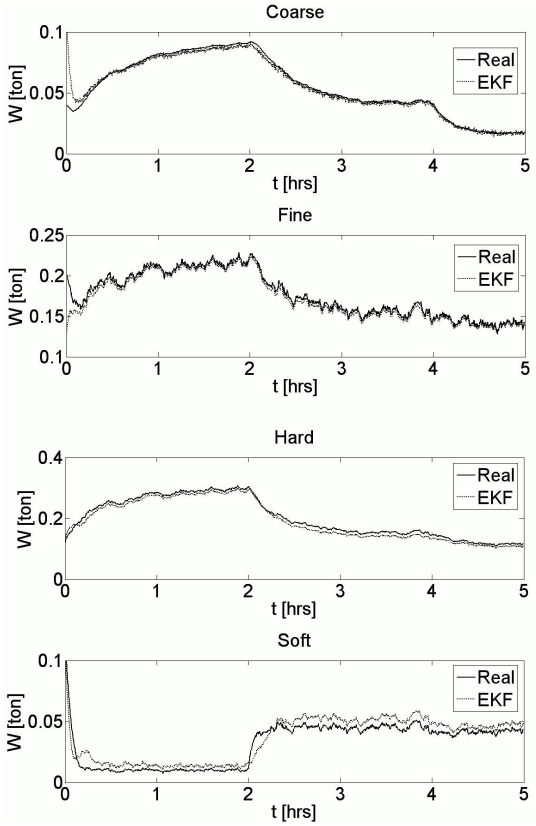

Fig. 6. State and joint state-parameter estimates with EKF.

90% to 95%. The state estimates results are displayed in figure 6 and the estimate of α is given in figure 7. Table 5 contains the estimation errors for different variations in α assuming the other parameters are constant. The case of figure 7, where initial α is 0.2 and final α is 0.4, generates an RMSE of 0.04.

Table 5: Error of parameter α.

α	0.1	0.2	0.3	0.4	0.5	0.6	0.7	0.8	0.9
0.1	0.17	0.16	0.06	0.05	0.12	0.08	0.10	0.11	0.14
0.2	0.16	0.10	0.03	0.04	0.07	0.07	0.10	0.11	0.13
0.3	0.16	0.05	0.02	0.03	0.06	0.06	0.11	0.11	0.15
0.4	0.15	0.05	0.04	0.03	0.04	0.07	0.13	0.15	0.42
0.5	0.54	0.41	0.42	0.24	0.03	0.06	0.13	0.12	0.13
0.6	0.58	0.41	0.41	0.23	0.05	0.08	0.14	0.13	0.14
0.7	0.48	0.45	0.43	0.27	0.07	0.07	0.07	0.06	0.07
0.8	0.60	0.46	0.43	0.26	0.05	0.07	0.05	0.04	0.04
0.9	0.66	0.48	0.42	0.26	0.13	0.06	0.04	0.03	0.02

The estimate of hardness using the state equations yields satisfactory results. The change in the proportion α was estimated correctly in many cases. Table 5 shows that approximately 65% of all combinations performed satisfactorily.

6. EVALUATION USING REAL DATA

6.1 Estimation of parameter α

The solution given in Section 5, though it performs successfully, assumes we have at our disposal an appropriately calibrated phenomenological model of the process. In an actual industrial plant, however, a model of these characteristics is not necessarily available. As we will now show, even in such situations it is possible to apply the same

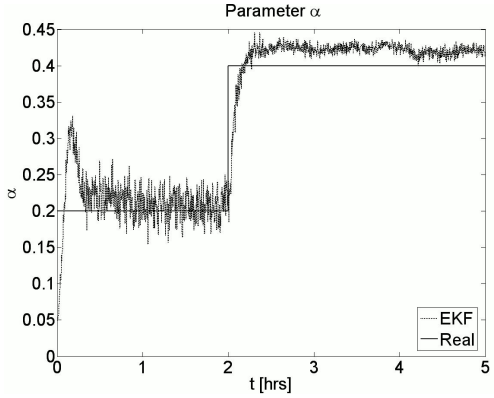

Fig. 7. Parameter α and α estimate.

concept of representing a change of hardness with a single parameter.

We begin by assuming we have identified two models $\mathcal{M}_1$ and $\mathcal{M}_2$ of extreme hardness. Let us also suppose that $\mathcal{M}_1$ and $\mathcal{M}_2$ present an ARMA model structure given by:

$$\mathcal{M}_1 : \ A_1(q)y(k) = B_1(q)u(k-d) \tag{12}$$

$$\mathcal{M}_2 : \ A_2(q)y(k) = B_2(q)u(k-d) \tag{13}$$

where A_1, A_2, B_1, B_2 are polynomials of orders n_a and n_b respectively, and q is an operator which represents a step forward in time, and d the delay of the model. We can express the two models in regresion form as:

$$\mathcal{M}_1 : \ y(k) = \phi_1^T(k)\hat{\theta}_1 \ ; \ \mathcal{M}_2 : \ y(k) = \phi_2^T(k)\hat{\theta}_2 \tag{14}$$

where ϕ_1^T, ϕ_2^T and $\hat{\theta}_1, \hat{\theta}_2$ are the regresion and estimated parameters vectors respectively. Let us now consider the case where the mill operates at an intermediate hardness. The integrated model then becomes:

$$\mathcal{M}_0 : \ y(k) = \alpha y_1(k) + (1-\alpha)y_2(k) \tag{15}$$

Where $y_1(k)$ and $y_2(k)$ are outputs of models $\mathcal{M}_1$ and $\mathcal{M}_2$ respectively. In order to determine parameter α, the following cost function is minimized:

$$J(\alpha) = \sum_{k=1}^{N} \left(y(k) - \alpha\phi_1^T(k)\hat{\theta}_1 - (1-\alpha)\phi_2^T(k)\hat{\theta}_2 \right)^2 \tag{16}$$

The optimal value $\hat{\alpha}$ that minimizes (16) is given by:

$$\hat{\alpha} = \left(\sum_{k=1}^{N} \psi(k)\psi(k)^T \right)^{-1} \sum_{k=1}^{N} \psi(k)z(k) \tag{17}$$

where $\psi(k)$ and $z(k)$ are given by:

$$\psi(k) = \phi_1^T(k)\hat{\theta}_1 - \phi_2^T(k)\hat{\theta}_2 \ ; \ z(k) = y(k) - \phi_2^T(k)\hat{\theta}_2 \tag{18}$$

One of the problems that arise in practice is to determine whether the operating situation corresponds to an extreme case of hard or soft ore. For this we propose the use of the average power-tonnage ratio, which intuitively represents how difficult it is for the mill to fracture the ore.

6.2 Test with industrial plant data

For testing the estimation algorithm, three series of normalized data obtained from measurements of a given industrial plant are used. Each series corresponds to plant

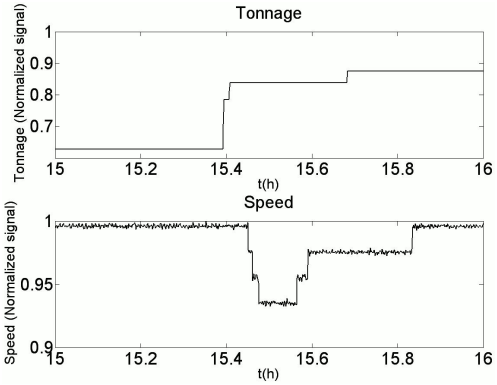

Fig. 8. Tonnage and speed inputs.

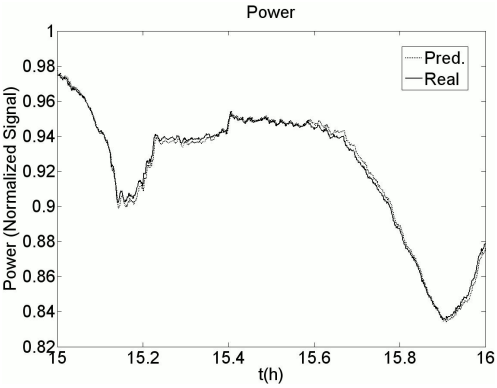

Fig. 9. Electric power and one step prediction of power.

operation on three different days. For the sake of simplicity, to identify the ARMA model, orders $n_a = 1$, $n_b = 1$ and $d = 0$ are employed.

The first base model is defined as the series with the lowest power-tonnage ratio ($\alpha = 1$), and the second base model as the series with the highest such ratio ($\alpha = 0$). From the third series, corresponding to the intermediate ratio, we use the first half to estimate parameter α, and the second half for evaluating the prediction with the integrated model. The error is evaluated by a one-step prediction with a sample period of $\Delta t = 2$. The signals are filtered by averaging the last ten samples. Figures 8 and 9 show the variation over time of the input and output variables, that is, tonnage set-point and mill speed, and electric power, respectively. Upon estimation of parameter α we obtain $\alpha = 0.67$, which indeed corresponds to an intermediate value between $\alpha = 0$ and $\alpha = 1$. For this parameter, the integrated model of power gives an RMSE of 0.007, far below 0.95 which is the average value of the normalized signal. The prediction obtained is shown in figure 9.

7. CONCLUSIONS AND FUTURE RESEARCH

The extended Kalman filter delivered similar state estimation results to the particle filter, although in some cases the latter was less robust. As regards robustness with respect to disturbances and estimation error, the EKF was heavily dependent on the matrices Q and R. The performance of the moving horizon estimator was acceptable, but was less precise than EKF and PF and exhibited higher computational costs, with execution up to ten times more time-consuming. This can be adjusted while maintaining reasonable results by changing certain parameters of the algorithm thanks to the flexibility provided by the genetic algorithms as an optimization tool.

The hardness estimation tests show that with a phenomenological model of the system, an extended Kalman filter delivers good results in a significant proportion of cases. Even in some of the cases with a relatively high error, the estimation still manages to detect the correct trend of the change in α. The approach based on summarizing the effects of an operational change in a single parameter is also useful if a model is not available. In this case, a very low error prediction error was obtained, by using an ARMA model.

As regards future research, the method presented here could be extended to models higher order and to applications other than semiautogenous grinding. The method could also be used in adaptive predictive control and in fault diagnosis.

REFERENCES

R. Amestica, G. Gonzalez, J. Menacho and J. Barria. A mechanistic state equation model for a semiautogenous grinding mill. *International Journal of Mineral Processing*, volume 44(45), pages 349–360, 1996.

S. Arulampalam, S. Maskell, N. Gordon and T. Clapp. A tutorial on particle filters for online non-linear/non-gaussian bayesian tracking. *IEEE Tansactions on Signal Processing*, volume 50(2), pages 174–188, 2002.

L.G. Austin. *Concepts in process design of mills, comminution practices.* Society for Mining, Metallurgy, and Exploration, Inc., Littleton, Colorado, 1997.

G.D. Gonzalez, R. Paut, A. Cipriano, D. Miranda and G. Ceballos. Fault detection and isolation using concatenated Wavelet Transform variances and discriminant analysis. *IEEE Tansactions on Signal Processing*, volume 54(5), pages 1727–1736, 2006.

J.A. Herbst, K. Rajamani and W.T. Pate. Identification of ore hardness disturbances in a grinding circuit using a Kalman filter. *Proceedings of the* 3^{rd} *IFAC Symposium on Automation in Mining, Mineral, and Metal Processing*, Montreal, pages 333–348, 1980.

C. Rao, J. Rawlings and D. Mayne. Constrained state estimation for nonlinear discrete-time systems: stability and moving horizon approximations. *IEEE Transactions on Automatic Control*, volume 48(29), pages 246–258, 2003.

D. Sbarbaro, J. Barriga, H. Valenzuela and G. Cortes. A multi-input-single-output smith predictor for feeders control in SAG grinding plants. *IEEE Transactions on Control Systems Technology*, volume 13(6), pages 1069–1075, 2005.

G. Welch and G. Bishop. An introduction to the Kalman filter. University of North Carolina, Chapel Hill, NC, Tech. Rep. TR-95-041, 2004.